A network model for learning-induced changes in odor representation in the antennal lobe

Michael Schmuker, Marcel Weidert, Randolf Menzel

A network model for learning-induced changes in odor representation in the antennal lobe

Michael Schmuker, Marcel Weidert and Randolf Menzel
Institute for Biology – Neurobiology
Freie Universität Berlin
Königin-Luise-Str. 28-30, 14195 Berlin
Germany
m.schmuker@fu-berlin.de, marcel.weidert@parexel.com, menzel@neurobiologie.fu-berlin.de

ABSTRACT

The antennal lobe (AL) is the insect homologue of the olfactory bulb in mammals. As such, it is the first processing station in the insect olfactory system. It has been shown previously that odorant representations change during associative odor learning [1], but contradictory findings have also been published [2].
We recorded Ca^{2+}-activity of uniglomerular projection neurons (PNs) in the AL of the honeybee *Apis mellifera* during differential olfactory conditioning.
Our results indicate that the activity pattern of PNs in response to odorants can change for the conditioned odor, for the unconditioned odor and for control odors which were not presented during conditioning.
We designed a computational model of the glomerular network that can explain the apparent contradiction between the findings we present here and the results reported in [2].

KEY WORDS
Olfaction, learning, neural coding, simulation.

1. Introduction

The honeybee exhibits remarkable performance in associative odor learning. Like Pavlov's dog learned to salivate in response to a bell ringing before food delivery, the honeybee can be trained to extend its proboscis when an odor is paired with a sucrose reward. Given the accessibility and comparably low complexity of its brain, the honeybee is therefore an ideal model for studying the neural basis of olfactory coding as well as learning and memory formation.
It has been shown in the honeybee that both the AL and the mushroom body (MB), the first and the second stages in the olfactory system, are involved in memory formation after olfactory reward conditioning [3]. Memory acquisition can be affected by local injections of octopamine (OA) into either one of the AL or MB [4]. OA is a neuromodulator which putatively gets released by the VUMmx1 neuron in response to sucrose reward [5].
Hence, associative learning is expected to have an effect on the plasticity of neuronal responses in the MB, but also in the AL. Indeed, Faber and coworkers have shown that Ca^{2+}-activity in response to an odorant increases for the learned odors, and that the correlation between response patterns for rewarded and unrewarded odors is reduced [1]. However, when Peele et al. analyzed odor responses of PNs (which form the output of the AL and project to the MB), they did not observe any significant changes in odor responses before, during and after conditioning [2]. Apart from the incongruity in experimental findings, it is also unclear how downstream neuron populations can be able to reliably identify odor stimuli when their representation in the AL changes.
In this contribution, we present data which supports the hypothesis that the glomerular activity pattern is changing. In addition, we provide a computational network model that can explain the apparent contradiction in experimental results. The model also resolves the problem how activity patterns can change in response to conditioning, while at the same time enabling downstream populations to reliably identify odor stimuli.

2. Results

2.1 Differential olfactory conditioning

We recorded Ca^{2+}-activity from uniglomerular PNs in the AL of harnessed honeybees during differential olfactory conditioning. We used four odors during our conditioning experiments: octanol, linalool, limonene and hexanal. In the pre-phase of each experiment, we presented each odor three times. For conditioning, we paired the presentation of one odor (the conditioned odor, CS+) with sucrose reward. Another odor (the unconditioned odor, CS-) was also presented in the conditioning phase, but was not paired with sucrose solution. CS+ and CS- were presented five times during the conditioning phase. In the post-phase, we presented the CS+, the CS- and the two remaining odors (Ctrl1 and Ctrl2) several times until the signal degraded.

2.2 Response patterns before, during and after differential conditioning

PN response was assessed as the integral of Ca^{2+}-activity during odor presentation. Depending on the preparation, 4 to 11 glomeruli were analyzed in an animal. Hence, the activity pattern in response to an odor was an n-dimensional vector, with n ranging between 4 and 11.

In order to visualize changes in the response patterns, we performed principal component analysis (PCA) on the n-dimensional response patterns. Fig. 1 shows the

scores of PN response patterns on the first two principal components (PCs) in one animal before, during and after conditioning.

The response pattern of the CS+ clearly shifts along PC 1. A similar shift can be observed for the CS-, although in a slightly different direction. The control odors (Ctrl1 and Ctrl2) also exhibit some shift, but to a lesser degree and in different directions. We observed similar shifts for the majority of 32 animals that we recorded from.

These observations indicate that response patterns of PNs are not invariant, but can be affected by olfactory conditioning.

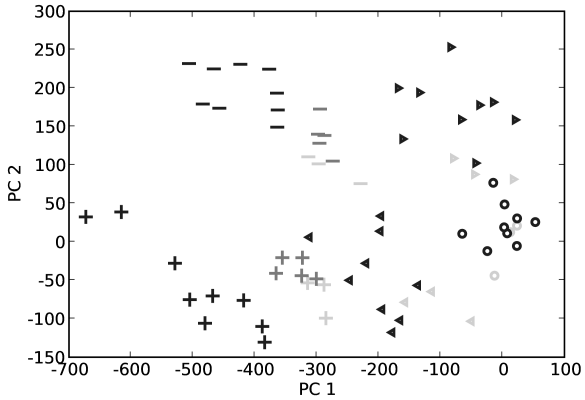

Fig. 1: Principal component (PC) scores for the first two PCs of PN response patterns before, during, and after conditioning. Symbols indicate the role of the odor (+: CS+, —: CS-, ◀: Ctrl1, ▶: Ctrl2), shades of gray show the phase of the experiment (▫: pre, ▪: training, ■: post).

2.3 A model of the glomerular network

Based on anatomical findings from the honeybee AL, we designed a model for glomerular network architecture that can resolve the apparent contradiction of our data with those from [2]. Since there are several PNs innervating each glomerulus [6], we formed the hypothesis that not all PNs inside a glomerulus respond with the same strength to upstream activity, but their responses can differ when a reward is delivered.

In consequence, measurements of Ca^{2+}-activity in a glomerulus could yield different results depending on the PN subpopulation that has been stained, probably because of a slight variation in the injection site or amount of injected dye. Sparser stainings may reveal differential effects that cannot be observed when staining all PNs inside a glomerulus, because the differences could average out.

Figure 2 shows a schematic of our model. An olfactory receptor neuron (ORN) drives two PNs, and two inhibitory local neurons (iLN and iLN-VUM). Both PNs also drive the iLN and receive recurrent inhibition from it. The PNs project their output to the MB. The VUMmx1 neuron (VUM) is active upon reward delivery and modulates the activity of a subpopulation of iLNs (iLN-VUM), which project to a subpopulation of PNs in the glomerulus.

This setting allows for the VUMmx1 neuron to modulate in an associative way the activity of PNs via the iLN-VUM. At the same time, the overall activity can be kept constant through action of the iLN – if PN2 decreases its activity, iLN activity decreases as well. PN1 will receive less inhibition and its activity can increase.

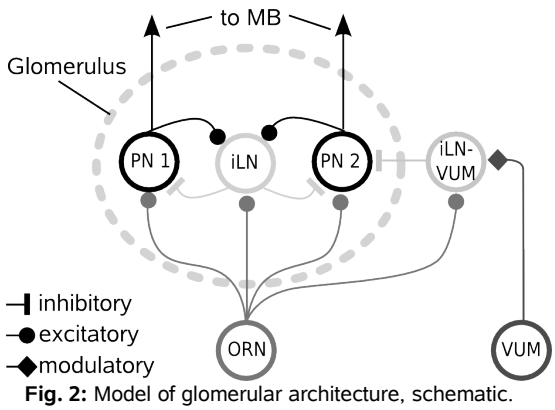

Fig. 2: Model of glomerular architecture, schematic.

In order to demonstrate the function of the proposed network, we implemented it using PyNN (http://neuralensemble.org/trac/PyNN). We used the `IF_curr_alpha` spiking neuron model (integrate-and-fire neurons with alpha-shaped postsynaptic currents); ORN firing was modeled as a poisson process, using PyNN's `SpikeSourcePoisson` model. Figure 3 shows spike trains from an exemplary simulation run. As proof of concept, we focused on the behavior of the network in the case that asymmetric PN activity is caused by activity of the VUMmx1 neuron when a reward is delivered, and did not yet consider plasticity in the network. Hence, the simulation only represented the action of the network during the conditioning phase.

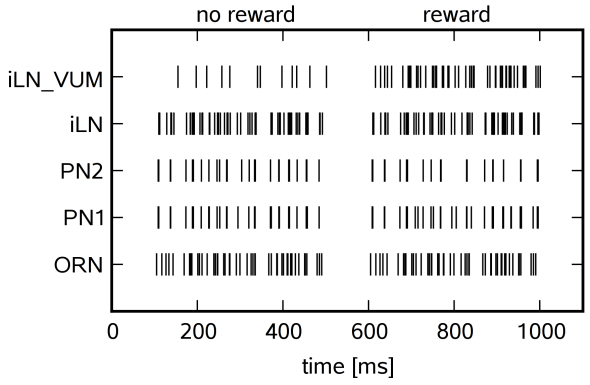

Fig. 3: Spike trains from one simulation run.

Two conditions are shown, with and without reward. We modeled the reward dependent modulatory activity of the VUM neuron as a decrease in firing threshold of the iLN-VUM unit. In the above example, the threshold was at -35 mV in the no reward condition, leading to 11 spikes being fired. When a reward was given, the threshold decreased to -55 mV, resulting in 54 spikes. In both conditions, the ORN delivered 46 spikes per odorant presentation. In the no-reward condition, PN1 fired 29 spikes while PN2 fired 26 spikes. But when the VUM-neuron was active in response to a reward, PN2 received more inhibition via the iLN-VUM and decreased its response to 21 spikes, while PN1 received less inhibition via iLN and increased its response to 33 spikes.

Hence, when averaging the response of PN1 and PN2, the response magnitude when reward is given (27.5 spikes) would be hardly distinguishable from the no-

reward condition (27 spikes). Only when analyzing PN1 and PN2 separately, the effect of reward presentation can be observed as an increase in asymmetry between PN responses.

The above scheme has also advantages when considering downstream neuron populations which should reliably identify the presented odor. If the signals of all PNs in one glomerulus are averaged, the response pattern is invariant to reward presentation. Simultaneously, the differential signal from PNs is available to indicate if the odor has been rewarded.

2.4 Adding plasticity to the model

So far, we only considered the effect of neuromodulation during the conditioning phase. As we have shown in section 2.2, appetitive conditioning causes changes in odor coding which outlast the conditioning phase. Hence there must be a mechanism which induces longer-lasting modifications of some synaptic weights.

For reward-based learning, both the input signal and the reward signal are required. In our model, both signals are available at the VUM-iLN: the ORN provides the input signal, while the reward signal is provided by modulatory input from the VUM neuron. If the synaptic weight between ORN and VUM-iLN is subject to plasticity, the VUM-iLN's odor response, and therefore its impact on odor coding by PN subpopulations, can be modified according to the temporal overlap between ORN input and reward signal. Hence, the synapse between ORN and iLN-VUM is the ideal location to induce synaptic plasticity during the conditioning phase.

Proper function of the network depends on the combination of synaptic weights. Not all weight combinations are equally well suited. If we introduce synaptic plasticity at a specific synapse, one weight is changing in an activity dependent manner. The remaining weights must be chosen such that a weight change at that single synapse is tolerated and does not jeopardize the function of the entire network.

We addressed this issue by scanning a large number of parameter combinations by their usefulness for the performance, or *fitness*, of the model. In a useful model, the average spike count of both PNs should stay as constant as possible in rewarded and unrewarded trials. We assessed this criterion by equation (1):

$$f_{\text{mean}} = \left| \frac{PN1_r + PN2_r}{PN1_{nr} + PN2_{nr}} - 1 \right| , \qquad (1)$$

with $PN1_r$ and $PN2_r$ the PN's spike counts for rewarded trials, $PN1_{nr}$ and $PN2_{nr}$ the spike counts for unrewarded trials, and f_{mean} the fitness criterion indicating how well the mean spike count from both PNs is preserved during rewarded and unrewarded trials.

In addition, the difference in spike counts should be small in unrewarded trials and large in rewarded trials. This was quantified by equation (2):

$$f_{\text{diff}} = \frac{1 + |PN1_{nr} - PN2_{nr}|}{1 + |PN1_r - PN2_r|} , \qquad (2)$$

where f_{diff} is the fitness criterion assessing how much PN responses diverge during rewarded trials.

Fitness increases if both criteria approach zero. The overall fitness f of a particular combination was calculated as

$$f = \frac{f_{\text{mean}} + f_{\text{diff}}}{2} . \qquad (3)$$

Table 1 displays the weights we used for probing the multidimensional "weight space". Negative weights indicate fitness assessment. We will use the abbreviations given in the third column for reference in the remainder.

Table 1: Weights used for fitness assessment.

source	target	abbr.	weights				
ORN	PN1, PN2	OP	20	25	30	35	40
ORN	iLN	Oi	2	4	6	8	10
PN1, PN2	iLN	Pi	6	8	10	12	14
iLN	PN1, PN2	iP	-20	-17.5	-15	-12.5	-10
iLN-VUM	PN2	iVP	-10	-8.5	-7	-5.5	-4
ORN	iLN-VUM	OiV	5	7.5	10	12.5	15

Our goal was to identify, out of all possible 15625 weight combinations, those in which OiV could vary the most with the least impact on model fitness. To this end, we assessed model fitness with each combination of weights from Table 1 for all values of OiV and calculated the mean and the variance of f. The ideal weight combination should exhibit small mean fitness, and low variance for different values of OiV. Figure 4 shows the distribution of mean fitness and its variance.

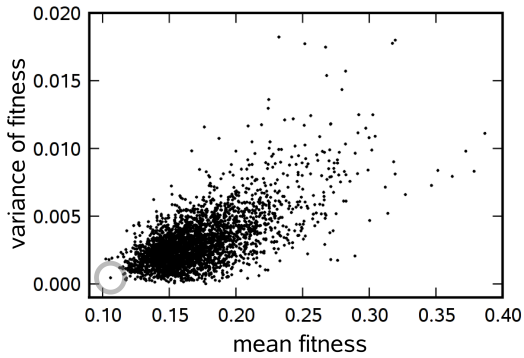

Fig 4: Mean vs. variance of fitness over different values of OiV. The gray circle marks the weight combination that we chose for the remaining simulations.

Most weight combinations yield good mean fitness around 0.15, with low variance around 0.02. For the remaining simulations, we chose the combination closest to the origin. The corresponding weight values were OP: 35, Oi: 6, Pi: 12, iP: -15, iVP: -4.

We enabled spike-timing dependent plasticity (STDP, [7]) at the synapse between ORN and iLN-VUM (OiV). Weights were modified in an additive manner using PyNN's `AdditiveWeightDependence` STDP rule with minimum and maximum weights $w_{\min} = 5$ and $w_{\max} = 15$. The maximum amount of weight change was bounded by $A^+ = 0.005$ for increasing and $A^- = 0.0025$ for decreasing weights. The temporal window for STDP was defined by $\tau_{\text{plus}} = 5$ ms and $\tau_{\text{minus}} = 7$ ms for potentiation and depression, respectively.

In order to mimic the data shown in 2.2, we organized our simulation runs into three phases: pre-, training- and post-phase, with 3, 5 and 3 trials respectively. The only difference between the phases is that during the training phase we lower the threshold of the iLN-VUM neuron to mimic a rewarded odor, in accordance to the model description in 2.3. Each trial was 500ms long, and trials were separated by intervals of 100 ms length during which no input activity was delivered. Figure 5 depicts spike trains from one simulation run.

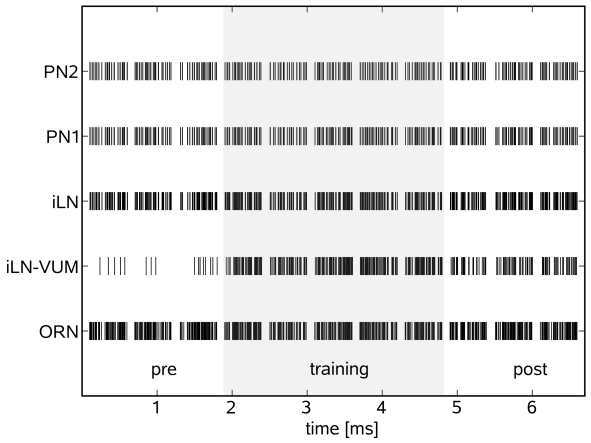

Fig. 5: Spike trains from one simulation run with plasticity. The gray rectangle marks the training phase, where the threshold of the iLN-VUM neuron is reduced.

In the pre-phase, the iLN-VUM neuron fired only few spikes, while in the training-phase its firing rate increased due to the decreased firing threshold, mimicking neuromodulatory input by the VUMmx1 neuron. In the post phase, the iLN-VUM exhibited an increased response to the stimulus as a result of the weight increase that has been brought about by STDP. In consequence of the increased iLN-VUM response, PN2 decreased its firing rate during the training- and post-phase of the experiment, while the response of PN1 increased.

This behavior can be observed more specifically in Figure 6, which shows the relative spike counts of PN1 and PN2 during the experiment.

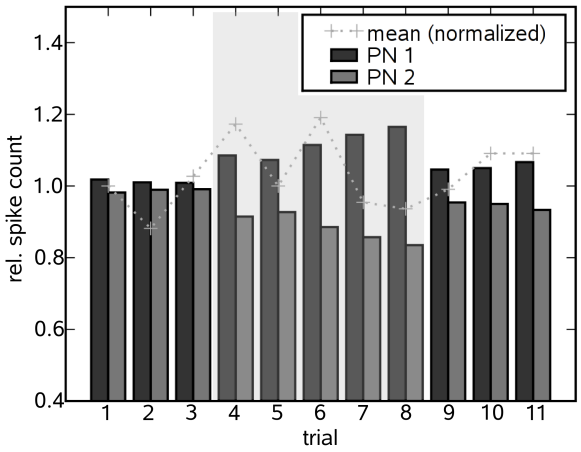

Fig. 6: Spike counts of PN1 and PN2, relative to the mean of both in each trial. Light gray crosses depict how the mean spike count varies, relative to the mean in trial 1. The gray rectangle marks the training phase.

In each trial, spike counts are scaled such that the mean spike count of both PNs equals one. In the pre-phase, there was only a small difference between spike counts from PN1 and PN2. During the training-phase, this difference increased and it was still large in the post-phase, demonstrating that synaptic plasticity at the OiV-synapse can effectively influence PN responses, making them inhomogeneous for rewarded odors. It must be noted that in the post-phase, the difference was somewhat smaller than during training, in slight incongruence with the original data. However, this incongruity could be addressed by using a different set of weights, which yield smaller, i.e. better values for f_{diff}, and thus a larger difference in the post-phase.

In order to demonstrate that average PN output actually stays the same, Figure 6 also depicts how the mean spike count evolved throughout the experiment. We normalized the mean values such that the value from the first trial equals one. Since the ORN input spike train is generated by a poisson process, it is subject to stochastic fluctuations, which are reflected by the variance in mean spike count over trials. In total, mean spike count was on the same level in the pre- and post-phase, with an apparent increase during the training phase.

In the above settings, the ORN always fired with with a spike rate of approximately 100 Hz. Because glomerular activity patterns are not all-or-nothing signals, but rather use the entire range of activities, we tested how the model performs for a range of input spike rates. Figure 7 depicts how the synaptic weight between ORN and iLN-VUM evolved for ORN rates between 10 and 130 Hz.

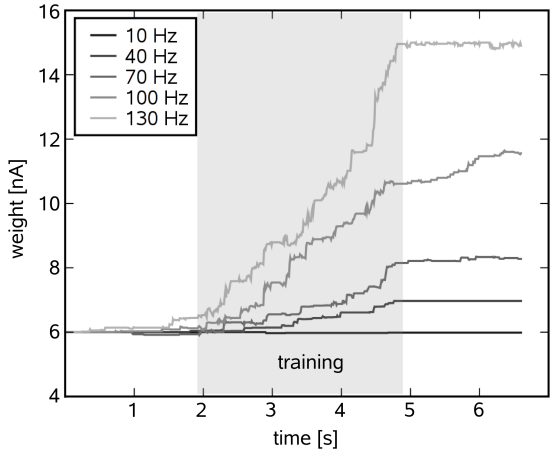

Fig. 7: Evolution of the weight between ORN and iLN-VUM for input rates between 10 and 130 Hz.

The higher the input rate, the more drastic was the change in synaptic weight. Hence, in multi-glomerular activity patterns, the glomerulus exhibiting the strongest response will change its response the most.

Another observation that can be made in Figure 7 is that the weight change is strongest during the training phase, and that there is relatively small or no change in the post-phase. This behavior indicates that the parameter setting we chose for the STDP rule is well suited to elicit synaptic potentiation mostly during training trials, and prevents that the weight changes erroneously during non-rewarded trials. However, it must be noted that for the largest input rate, the synaptic weight is “maxed out”, so no further potentiation can take place. Possibly, this behavior could be avoided by tuning the parameters

of the STDP mechanism, or simply avoiding the use of input rates higher than 100Hz in the model.

3. Conclusion

We presented data showing changes in the representation of odorants in the AL induced by olfactory associative learning. These data conflict with previously published findings, and also raise the question how downstream neurons can identify odor stimuli when their representation in the AL is changing. Proposing a connectivity scheme for glomeruli that can resolve that conflict, we constructed a computational model of the glomerular network, in which the response of PNs in one glomerulus is not homogeneous, but diverges when an odor is rewarded or associated with a reward. In a computational conditioning experiment, we employed STDP at one synapse in the network to acquire this assymetry in PN response during the training-phase when odor presentation is paired with activity in the VUMmx1 neuron (i.e., when the odor is rewarded), and showed that it was preserved in later trials without VUM activity.

We showed that the network model is capable of generating asymmetric PN responses, while at the same time keeping the average response relatively constant. Hence, downstream neurons could obtain reliable information about the stimulus by integrating the signal of all PNs from one glomerulus, or obtain information about which odor was rewarded by analyzing the differential signal.

The model makes the prediction that responses of PNs in the same glomerulus are not homogeneous when odors are rewarded. This prediction can be tested experimentally, e.g. by recording the activity of PNs belonging to the same glomerulus during olfactory conditioning.

The experimental data provides us not only with data from one glomerulus, but from several glomeruli giving the entire activity pattern in the frontal aspect of the antennal lobe in response to odorants. Our goal is to use several model glomeruli in order to reproduce our experimental findings and analyze the effect of plasticity in the antennal lobe on odorant response patterns.

References

[1] T. Faber, J. Joerges, & R. Menzel, Associative learning modifies neural representations of odors in the insect brain, *Nature Neuroscience*, *2*(1), 1999, 74-78.

[2] P. Peele, M. Ditzen, R. Menzel & C.G. Galizia, Appetitive odor learning does not change olfactory coding in a subpopulation of honeybee antennal lobe neurons, *Journal of Comparative Physiology A*, *192*(10), 2006, 1083-1103.

[3] R. Menzel & M. Giurfa, Cognitive architecture of a mini-brain: the honeybee, *Trends in Cognitive Sciences*, *5*(2), 2001, 62-71.

[4] M. Hammer & R. Menzel, Multiple sites of associative odor learning as revealed by local brain microinjections of octopamine in honeybees, *Learning & Memory*, *5*(1-2), 1998, 146-156.

[5] M. Hammer, An identified neuron mediates the unconditioned stimulus in associative olfactory learning in honeybees, *Nature, 366*, 1993, 59-63.

[6] J. Rybak, *Die strukturelle Organization der Pilzkörper und synaptische Konnektivität protocerebraler Interneuronen im Gehirn der Honigbiene, Apis mellifera* (Ph.D thesis, Freie Universität Berlin, 1994).

[7]G. Bi & M. Poo, Synaptic modification by correlated activity: Hebb's postulate revisited, *Annual Review of Neuroscience, 24*, 2001, 139-166.